A Study of the Sensitivity of the IceCube Detector to a Supoernova Explosion

---

A Thesis

Presented to

the Faculty of the Graduate School

Southern University

In Partial Fulfillment

of the Requirements for the Degree

Master of Science

---

by

Aaron Simon Richard

August, 2008

This research was supported by the a MRE grant from the National Science Foundation through a subcontract from the University of Wisconsin Board of Regents under the contract No. G067933

A Study of the Sensitivity of the IceCube Detector to a Supoernova Explosion

---

An Abstract of a Thesis

Presented to

the Faculty of the Graduate School

Southern University

In Partial Fulfillment

of the Requirements for the Degree

Master of Science

---

by

Aaron Simon Richard

August, 2008

ABSTRACT

The IceCube neutrino telescope under construction at the South Pole, consists of 4800 Digital Optical Modules (DOMs) attached to 80 vertical 1-km long strings arranged in a hexagonal shape. Each string contains 60 DOMs located at a depth of 1450-2450 meters under the ice. The total instrumented mass will be approximately one gigaton of ice. On the surface, the IceTop air-shower detector array is composed of 320 DOMs. This neutrino observatory will open an unexplored view of the universe spanning the energy range of 10^7 - 10^{15} eV. This makes it possible to search for low energy neutrino bursts from supernova (SN) core collapse. An extremely large number of positrons and electrons resulting from Charged Current (CC) interactions of $\bar{\nu}_e$'s and ν_e's on H and O nuclei will be detected by the DOMs using the Cherenkov light produced by these low energy particles in the IceCube Detector. A special SN trigger based on a 5.5σ excess on top of the dark count-rate background in the DOMs would alert the experiment to a possible SN explosion. The IceCube detector, electronics and the methods used to search for SN candidate events are discussed. A Monte Carlo (MC) simulation for data comparison and for signal prediction is presented [1].

ACKNOWLEDGMENTS

First the author would like to thank the Physics Department at Southern University for believing in him and giving him the opportunity to pursue his interest and goals in the area of particle physics.

He would like to thank Dr. Chia Yang for understanding him and introducing him to this wonderful world of Physics. For without his encouragement and guidance the author would simply have become just an engineer.

Sincere thanks to all of the faculty: Dr. P.M. Lam, Dr. D.S. Guo, Dr. J.D. Fan, and Dr. R.M. Gnashingha, for the guidance and the skills they have taught him to assist with his educational endeavorers. His time spent in the department has been an enjoyable one thanks to these marvelous men of science.

Also Dr. Samvel Tear-Antonyan for answering questions about programming and explaining a lot of "How do I do this?" questions. Because without him the author would have been lost. Furthermore, thanks to Dr. Richard L. Imlay for his valuable comments and suggestions regarding this thesis.

Most of all, the author wishes to recognize Dr. Ali Reza Fazely for his tireless understanding and patience, painstakingly explaining theory,

and exceptional guidance without which none of this would be possible. Additionally to Dr. Fazely thanks for just believing in him and motivating him to believe in himself.

TABLE OF CONTENTS

LIST OF TABLES

LIST OF FIGURES

CHAPTER I

INTRODUCTION

I.1 Statement of the Problem

We investigate the detection of supernovae in our universe using neutrinos. The IceCube high energy neutrino observatory for astrophysics is able to search for low energy neutrino bursts from the core collapse supernovae. A large number of positrons originating from a large flux of $\bar{\nu}_e$ would induce an excess on the counting rate above background in all digital optical modules (DOMs). The detector characteristics and methods used to search for burst candidates in addition to the different isotopes found in IceCube will be discussed. The cross sections for different interactions of neutrinos on the isotopes in IceCube are addressed. With the low noise rates in IceCube, it can be determined with great precision that a common rise in PMT activity will be associated with a neutrino burst uniformly illuminating the ice.

In August of 2007 the IceCube SN read-out began recording data in search of such events. The DOM rates are summed in time intervals of 2ms. To rebin and align the rates of individual modules, a histogramming program was written by the IceCube collaboration, along with an analysis program used to clean, test, and record the events. Depending on the year of data taking the IceCube coverage will be 100% of supernova in our galaxy. This supersedes its

predecessor, the Antarctic Muon and Neutrino Detector Array (AMANDA) detector, which only covered 70-92% of our galaxy. The significance of observing supernova neutrinos in Super-K and/or the Large Volume Detector (LVD) can be enhanced and complemented by a simultaneous of observation in the IceCube detector due to its excellent time resolution and lack of low energy trigger requirements. IceCube is a memeber of the SuperNova Early Warning System (SNEWS).

I.2 Motivation for this Work

The motivation behind this study is to search for supernovae with the IceCube neutrino telescope. We intend to study several cross section calculations for the $\bar{\nu}_e p \rightarrow n e^+$ reaction. This neutrino interaction dominates all other reactions in a SN explosion and can be detected by the IceCube detector. The cross section calculations are the only tools available at this energy range for sensitivity estimates of IceCube to a possible SN explosion. This cross section cannot be measured experimentally in the range of neutrino energies produced in a SN. With these calculations we intend to determine the sensitivity of the IceCube detector.

I.3 Organization of Remainder of this Thesis

This thesis is divided into five chapters, in order to provide a comprehensive understanding of the detection of supernova with the IceCube Neutrino Detector

Chapter One is the introduction and statement of the problem. Also here we discuss the motivation for this work and give a brief description of the contents of this thesis.

Chapter Two is a detailed description of Supernova and neutrinos.

Chapter Three is there is a discussion of the experimental setup and description of the IceCube detector.

Chapter Four contains the discussion of the neutrino intensity and abundance of isotopes found in IceCube. An analysis of cross section calculations by different authors used to calculate the sensitivity of the IceCube detector is described.

Chapter Five contains the discussion of the results.

CHAPTER II

SUPERNOVA DESCRIPTION

II.1 Type II Supernovae

It is estimated that every 30 years or so in our galaxy a massive star with a mass $M > 8M_{\odot}$ explodes. Here $M_{\odot}$ is the solar mass and it is equal to 1.98892×10^{30} kg.[6] More massive stars with mass more than $8M_{\odot}$ spend only millions of years expending their H fuel. That is fusing hydrogen nuclei into helium nuclei. This stage is called the main sequence. After all the hydrogen in the central regions of the star is converted into helium, the star will begin to burn helium into carbon. This exhaustion of its fuel continues through heavier elements until a massive iron core is formed. Figure II.1

Iron is unique for it has the highest binding energy per nucleon in the periodic table. Nuclear fusion of nuclei that are heavier than Fe are not accompanied with energy release and, on the contrary require additional energy. Therefore Fe fusion process will not begin, the daughter element in this process is less stable than Fe. As a matter of fact, all trans-iron elements are less stable than Fe and therefore, the Si-Si fusion would be the end cycle before the SN explosion. When fusion stops there is nothing to combat the force of gravity on the outer layers and this results in the collapse and death of the star. The lack of radiation pressure causes the outer layers of the star to fall inward. During this core collapse, which happens in about 15 seconds,

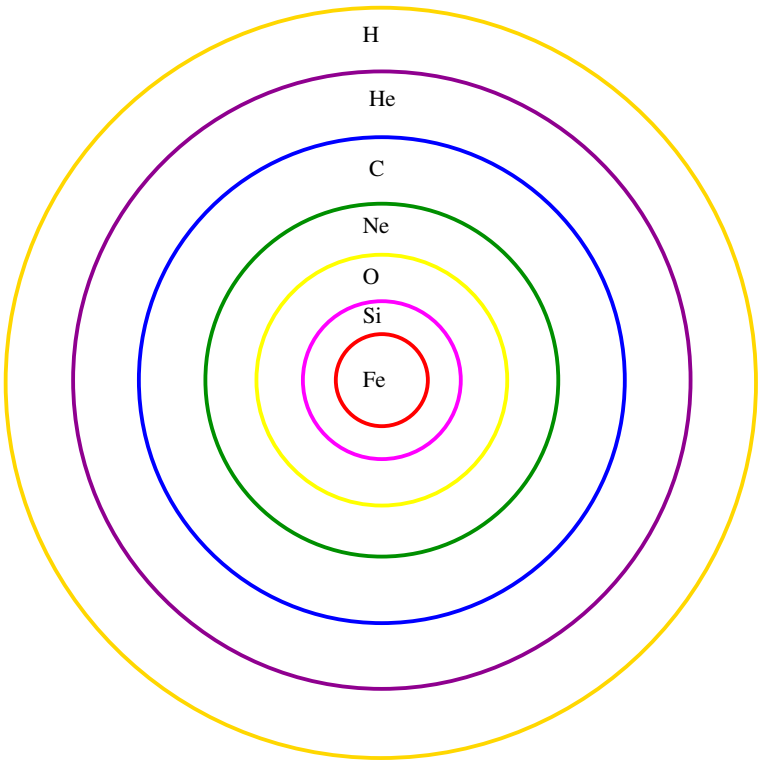

Figure II.1: Graphical representation of the order in which a Star expends its fuel.

the nuclei in the outer parts of the star are pushed very close together, so close in fact that other elements heavier that iron are created. Stars that are between 5 and 8 times the mass of our sun form neutron stars during implosion. Stars with masses greater than 10 times the mass of the Sun will not form neutron stars but instead will create black holes. A neutron star or a black hole is formed when a supernova explosion occur. This cataclysmic explosion sends all stellar material deep into the stellar medium. We patiently wait with great anticipation for the next phenomenal event that will light up our night sky. Figure II.2 shows what happens during the core collapse of

the star just before its explosion.

Because of the pressure created by the infalling material the weak interaction dominates the evolution of the neutron star. The neutrino emission from the core efficiently removes entropy from the star, ultimately causing the iron to have a very low entropy per baryon. The iron core is supported by relativistically degenerate electrons that have certain implications: the iron core will then go unstable and collapse at a near free fall rate on a very low adiabatic slope until nuclei and nucleons merge at nuclear density. After that a shock wave is generated at the edge of the inner homologous core i.e. the same chemical composition. During the collapse the electron Fermi energy rises as the volume of the core decreases. Electron capture on protons goes up lowering the fraction of electrons per baryon, which ultimately lowers it to the Chandrasekhar mass ($1.4M_{bigdot}$). Because of the low entropy most of the protons available for capture by the electrons are bound in the nuclei.

During this evolutionary process the gravity associated with the stability of the core becomes so massive it overcomes the electron pressure due to coulomb repulsion then the collapse begins. This results in an increasing nuclear density as the core's radius decreases until a radius of R = 10km is achieved. With $E = 3/5GM^2/R \sim 10^{59}$ MeV the core collapses and all the neutrinos are trapped in the neutrino-sphere as the materials bounce around in the core. Then just before the imminent destruction of the star emission

of the neutrinos occurs, the Shock wave is next then the explosion. The binding energy $E_{kin} \approx 0.01E$ of thetotal energy of the star therefore, 99% of this energy is carried off by the neutrinos.[6]

Just before core collapse the dominant reaction that control the n/p ratio are the capture reactions on free nucleons inside the "neutrinosphere"

$$\nu_e + n \leftrightarrow p + e^- \tag{II.1}$$

$$\bar{\nu_e} + p \leftrightarrow n + e^+ \tag{II.2}$$

During the neutrino mixing and nucleosynthesis process in core collapse SN, a variety of interesting phenomena occur. The electron-positon and neutrino pair annihilation processes which produce muon and tau neutrino pairs are represented by the following equations:

$$\nu_e \bar{\nu_e} \rightarrow \nu_{\mu,\tau} \bar{\nu}_{\mu,\tau} \tag{II.3}$$

$$e^+ e^- \rightarrow \nu_{\mu,\tau} \bar{\nu}_{\mu,\tau} \tag{II.4}$$

After studies aynd Janka [11] the first equation has been determined to be a more dominating source for the production of muon and tau neutrino pairs. Because the energies of the muon and the tau neutrinos and anti-neutrinos produced are too low to produce charged leptons, these neutrinos interact only with the neutral current interactions (NC). These particles will also remain in a local thermal equilibrium as long as they can continue to

interact with other particles and exchange energy and enjoy neutrino pair creation or annihilation.

It has determined that the neutrino bremsstrahlung process [15]

$$N + N \leftrightarrow N + N + \nu\bar{\nu} \tag{II.5}$$

is more effective than the annihilation process described above in creating a high neutrino number density although the neutrino-antineutrino annihilation process $\nu_e\bar{\nu}_e \leftrightarrow \nu_{\mu,\tau}\bar{\nu}_{\mu,\tau}$ is one of the major sources of muon and tau neutrinos.[11]

II.2 Neutrinos

The "desperate remedy then assumed" [5] was first introduced in 1930 by Wolfgang Pauli as a solution to the problem found with the the assumed wo body process of beta decay where there was an apparent discrepancy with the conservation of energy, conservation of momentum, and spin. When a neutron was assumed to decay into a proton and electron there was no explanation for the energy loss. Pauli theorized that there was an undetected particle carrying away the missing momentum, energy and spin, turning the two body process into a three body process. If this was to be correct the particle had to have no charge, have a rest mass equal to or less than the rest mass of the electron (.511 MeV), and also like the electron it must posses an

intrinsic spin of $\frac{1}{2}\hbar$. In addition to these basic properties the neutrino also had to obey Pauli's exclusion principle; which is, no two identical neutrinos can be in the same quantum state at the same time.

Enrico Fermi developed the first theory describing neutrino interactions and he is credited with giving the particle its name "neutrino" which means little neutral one. It was not until 1956 that Fredrick Reines and Clyde Cowan first detected the neutrino and Reines was awarded the Nobel Physics prize in 1995 for their discovery.

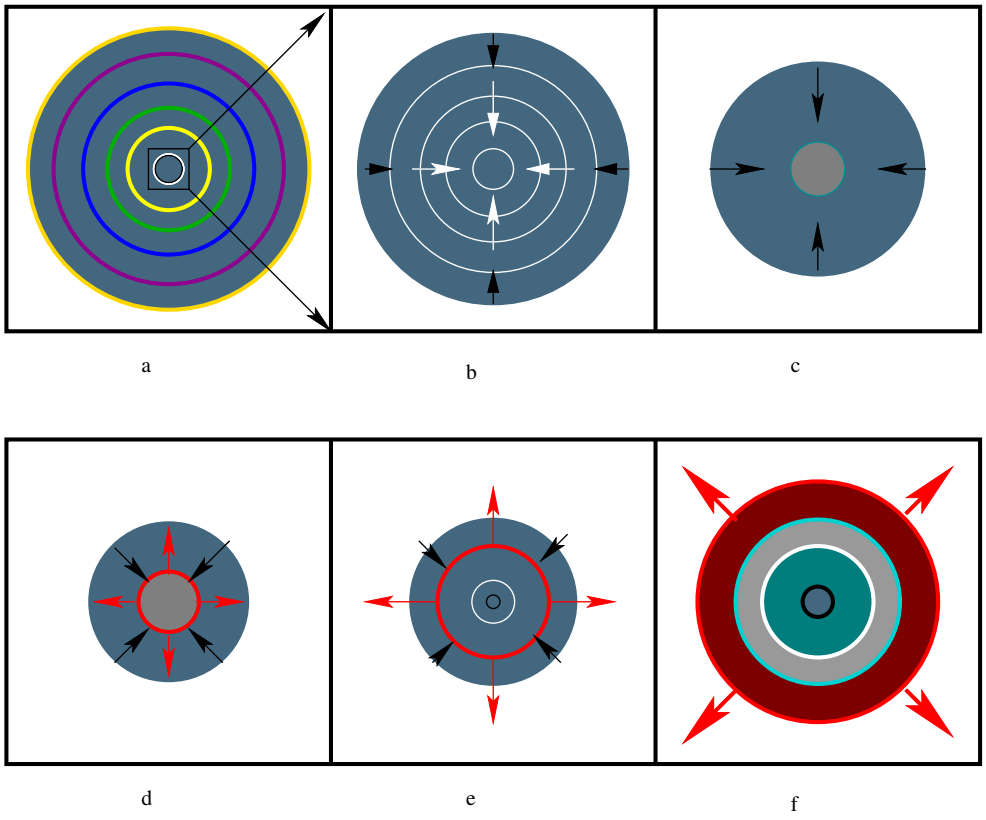

Figure II.2: A graphical depiction of what happens during the collapse phase inside a massive, evolved star (a) the onion-layered shells of the elements undergo fusion, consequently forming an iron core (b) that reaches Chandrasekhar-mass ($1.4M_{bigdot}$) and then begins to collapse. The inner part of the core is compressed into neutrons (c), causing the infalling material to bounce and cool the star (d) and form an outward-propagating shock front (red). The shock starts to stall (e), but it is re-invigorated by neutrino interaction. Resulting in the surrounding material being blasted away (f), leaving only a degenerate remnant.

CHAPTER III

EXPERIMENTAL ARRANGEMENT

III.1 The IceCube Neutrino Telescope

A great number of areas in the universe are inaccessible to study using other types of cosmic rays and E-M radiation that reach the earth. The high-energy photons are absorbed by the Cosmic Microwave Background radiation (CMB), and protons do not carry directional information because of their deflection by the magnetic field of the Galaxy. This renders neutrinos the most suitable candidates to study the structure of the universe and cataclysmic events therein. This elementary particle travels close to the speed of light, it is electrically neutral and only carries the weak interaction. Also neutrinos have a very low reaction cross section which allows them to pass through ordinary matter almost undisturbed.

The IceCube neutrino detector is being constructed at the South Pole. It is able to detect the interactions of neutrinos as they propagate through the ice interacting with H and O nuclei in the IceCube Detector. To give an idea of the IceCube geometrical size refer to the figure III.1.

The minimal supersymmetric model generally predicts the neutralino as

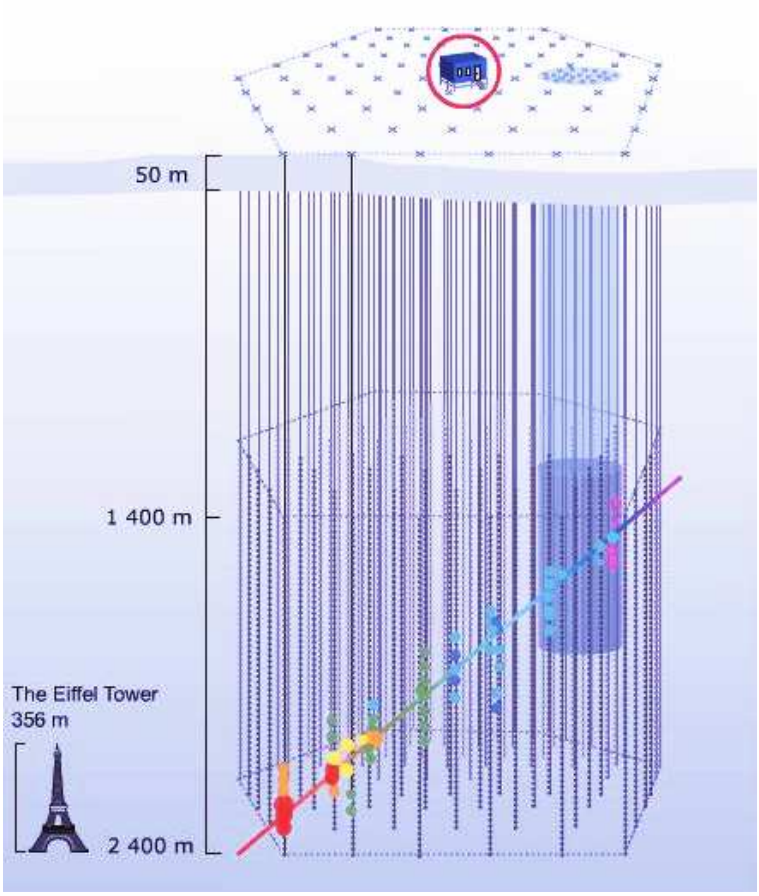

Figure III.1: Schematic drawing of IceCube using Eiffel Tower as a reference for its size. Also a particle being detected as it passes through IceCube.

a prime candidate for cold dark matter. IceCube is sensitive to cold dark matter particles, usually refered to as Weakly Interacting Massive Particle (WIMP) with a mass approaching TeV. IceCube offers numerous discovery possibilities including being sensitive to supernova within our galaxy and beyond. It is capable of detecting neutrinos with energies far above those produced at accelerators.

III.2 The IceCube detector

The IceCube In-Ice detector, located at the Geographic South Pole, shown in Fig. III.2 detects high energy neutrinos that traverse the earth and interact deep in the ice below the South Pole.

Figure III.2: IceCube Located at the South Pole, Antarctica

Particles produced by charged or neutral-current neutrino interactions generate Cherenkov light that can be detected by an array of photomultiplier tubes (PMTs), refered to as digital optical modules (DOMs) shown in Fig. III.6. We desicrbe later in this chapter what a DOM is. Extremely deep water filled holes are created by melting the ice with hot water drills and then strings of DOMs are lowered into the water filled holes (see Fig. III.3). This process will be repeated until the grid is complete. The AMANDA

detector which was completed in 2000 and has a total of 677 DOM's on 19 vertical strings served as a "proof of concept" for the IceCube detector. IceCube is a much larger and more sophisticated detector composed of 4800 optical modules deployed on vertical strings buried 1450 to 2450 meters under the surface containing a volume of $1km^3$ of the ice. Each string contains 60 DOMs spaced 17 m apart.

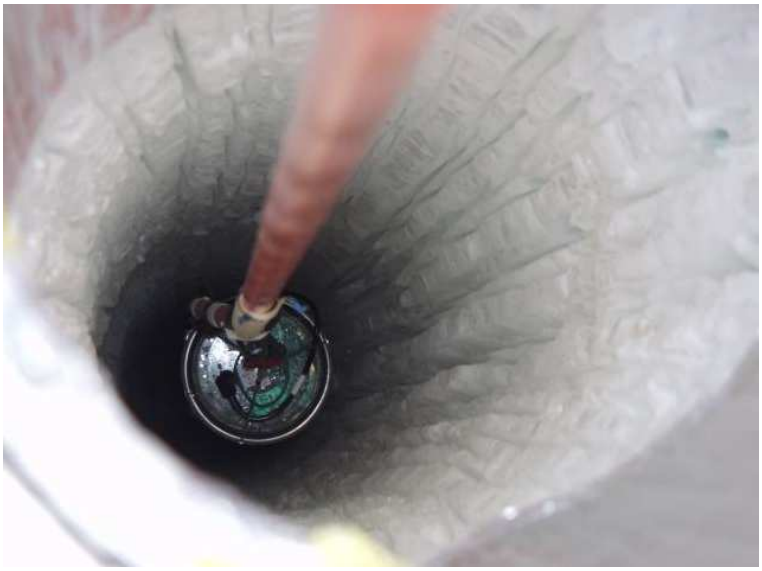

Figure III.3: Actual DOM being deployed

III.3 IceTop

Also a surface air shower detector array, IceTop, is comprised of 320 optical modules. The surface air-shower array is housed inside two detector tanks each above an in-ice string. As shown in Fig. III.4 and Fig. III.5, each

2.7m diameter ice filled tank contains two DOMs. As well as serving as an air-shower detector IceTop can be used to help calibrate IceCube and as a veto for IceCube.

Figure III.4: The IceTop detector setup

The relativity sparse distribution of PMTs is ideal to IceCubs's primary interest in having a sensitivity for neutrino energies above 1 TeV. The first string was deployed in January 2005 and 21 more in the following two austral summers. These strings are operating well and construction is on schedule for completion of IceCube in 2011. Each DOM, as shown in III.6, consists of a 13-inch diameter pressure vessel containing a Hamamatsu R7081-02 10-inch diameter PMT, PMT base, high voltage supply and signal processing and calibration electronics. The trigger and front-end electronics are located on

Figure III.5: The IceTop detector tanks

the main board. Also enclosed are two analog-to-digital converter (ADC) systems, a precision clock and a large Field Programmable Gate Array (FPGA) for control and communications. All communications with the surface are through a single twisted pair shared by two DOMs. This single pair carries power, bi-directional data and timing calibration signals.

The PMT signal is sent to a discriminator and two separate digitizer circuits. The firing of the discriminator, typically set for 1/3 of a photo-electron pulse, initiates a digitization cycle. The first digitization provides 14 bits of resolution based on a switched-capacitor-array chip. The other digitizer system detects late arriving light which has scattered in the ice. A second board holds 12 Light Emitting Diodes (LED) that are used for calibration. Half of the LEDs point horizontally outward while the other

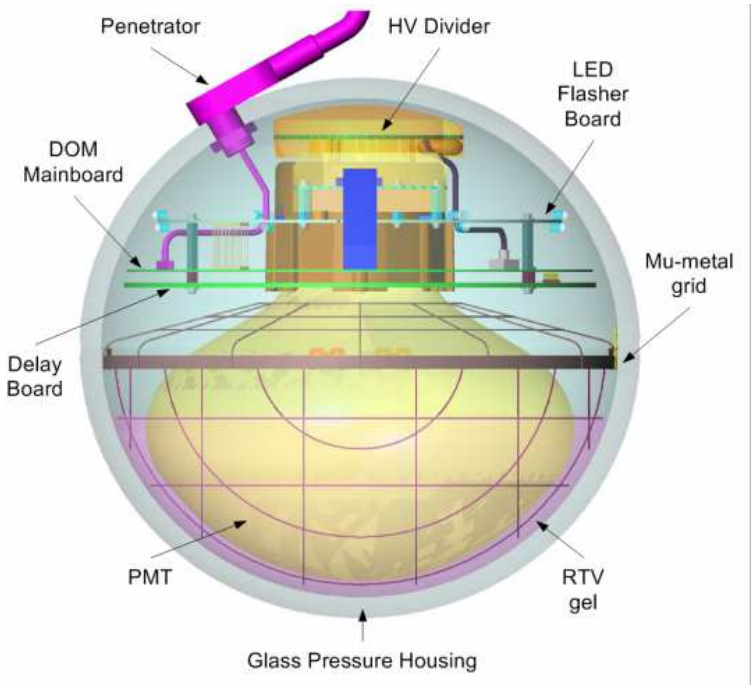

Figure III.6: Schematic cross section of a DOM

half point upwards at 45 degrees.

Modeling the performance of IceCube depends crucially on a detailed understanding of the optical properties of the ice. Data was taken by AMANDA using various pulsed and continuous light sources. AMANDA has mapped scattering and absorption of light to study the optical properties of the glacial ice at the South Pole for wavelengths between 313 and 560 nm at depths between 1100 m and 2350 m [8]. As much as a factor of seven variations for scattering in the depth range of the IceCube DOMs was observed. A notable observation concerning the ice properties is the ice has

a very long absorption length, typically 100 m while the effective scattering length is short, typically 20 m. For comparison, in water detectors such as ANTARES the scattering lengths are long (almost 100m) and absorption lengths are short (almost 20m) [10].

The scattering of light in the ice is strongly forward peaked so that several scattering events are needed to substantially change the direction of the photon. Therefore when looking at the effective scattering length, $L_{(eff)} = L_S/(1- < \cos\Theta >)$ where L_S is the mean distance between scatters and $< \cos\Theta >$ is the average cosine of the angle of scatter. Qualitatively speaking, $L_{(eff)}$ is the distance required to substantially change the direction of the photon. It can be shown that scattering is described very well by the single parameter, $L_{(eff)}$ for large distances compared to $L_{(eff)}$. The light that reaches a DOM typically do not take the shortest path to the DOM and thus arrives delayed by a time, $t_{(residual)}$. Fitting procedures use this time information as well as the pulse heights. For high energy muons in AMANDA the direction can be determined to less than two degrees and the energy to 0.4 in $log_{(10)}\frac{E}{GeV}$.[8]

III.4 GEANT Simulation

Graphical representation to the GEANT-3.21 simulation as a function of depth is shown in the figure III.7. The inefficient region of the IceCube

detector is represented by the apparent dip in the graph. This drop in efficiency is believed to be caused by "dirty" ice resulting from volcanic ash being deposited there from an erupting volcano during the time the layer was formed. This can be confirmed by examining the graph around string 37 and at a depth of 2,050 m. This is consistant with the atmospheric muon data.[9] Also shown in Fig. III.8 are the detected events from a 10 million event simulation. The areas that contain a more concentrated number of events simply coincide with the string of DOMs that are located there.[1]

IceCube's angular resolution for muons is approximately one degree at high energies. Electromagnetic and hadronic showers are short, normally 10 to 20 meters. This results in inaccurate directions in AMANDA up to 30 degree, but containment allows a better energy measurement (30%) than for muons. Similar to AMANDA, IceCube has an energy threshold around 100GeV. The trigger rate is approximately 80 Hz which is similar for both IceCube and AMANDA where all events with 24 DOMs firing within 2.5 μsec are recorded. This procedure yields around 10^9 events each year, primarily going down muons arising from decays of π's produced by cosmic rays interactions in the atmosphere above the detector. Approximately 10^6 of these down-going muons are mis-reconstructed as up-going muons. The primary physics sample of AMANDA consists of approximately 10^3 up-going muons produced per year by neutrinos that traverse the earth and interact in the ice in or near the detector. Very elaborate software is required to reduce the muon background to an acceptable level by cutting out the poorly

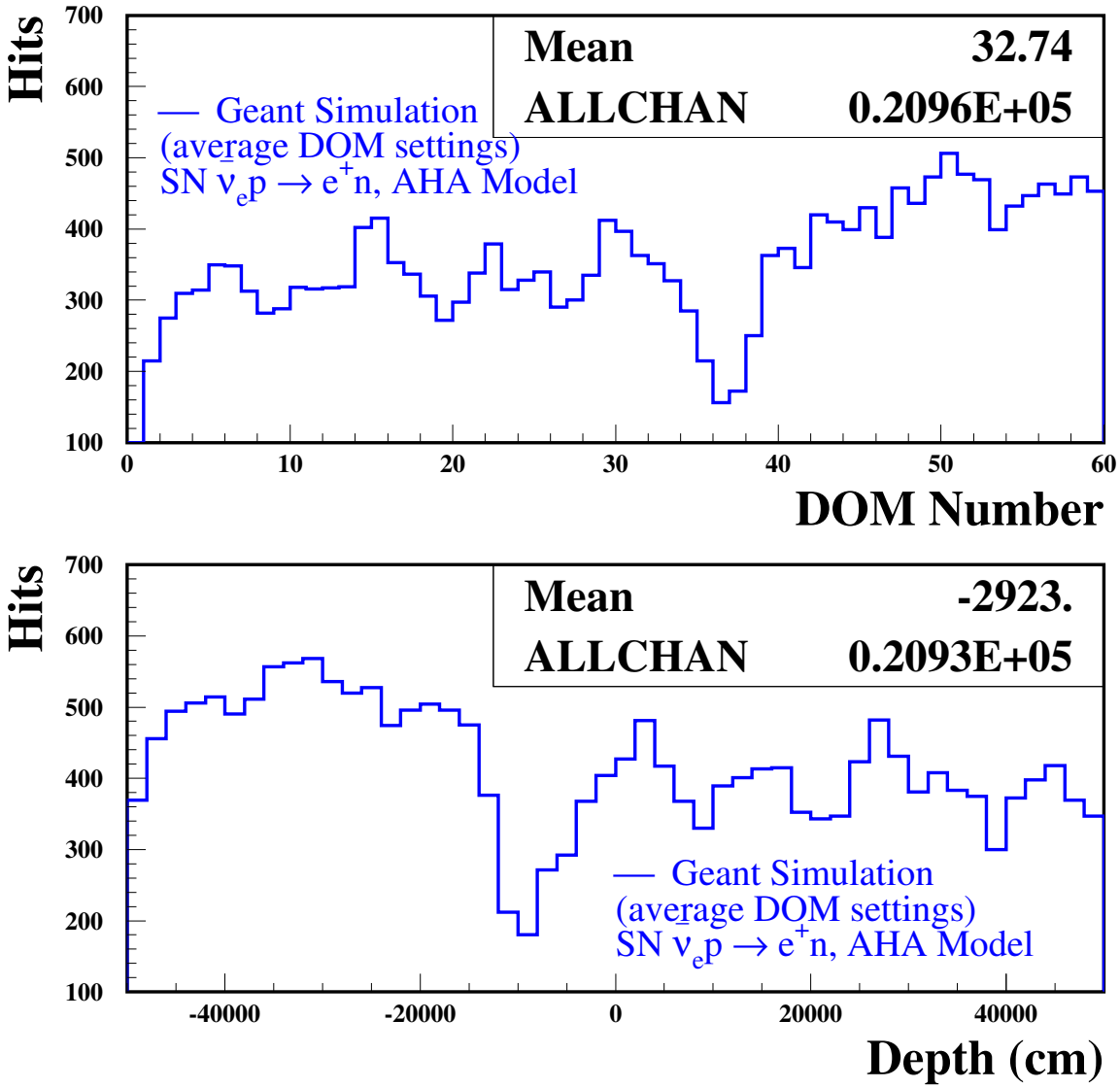

Figure III.7: These graphs represent the number of hits experienced by the DOMs as a function of depth.

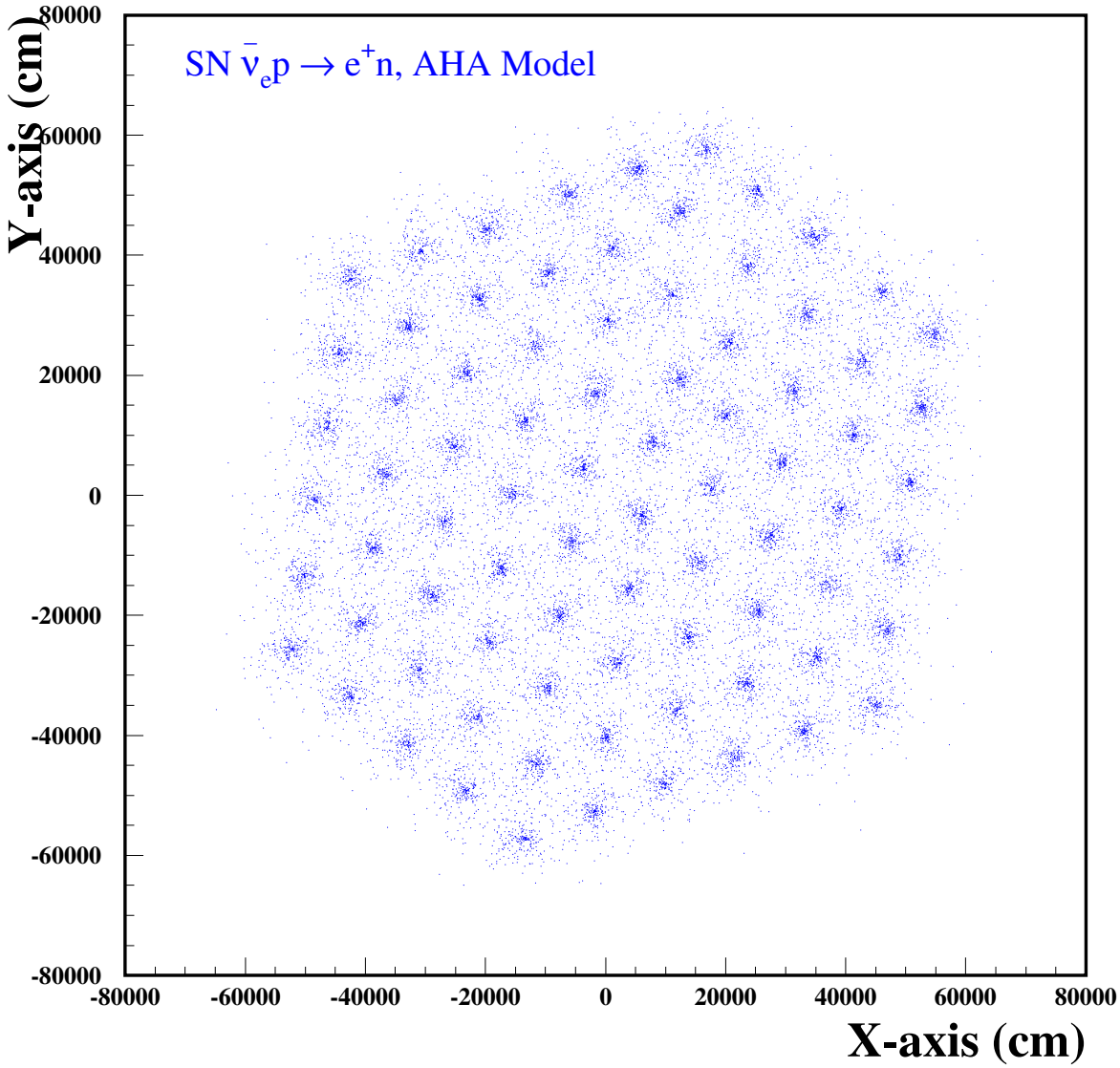

Figure III.8: Graphical representation of GEANT-3.21 10 million event simulation.

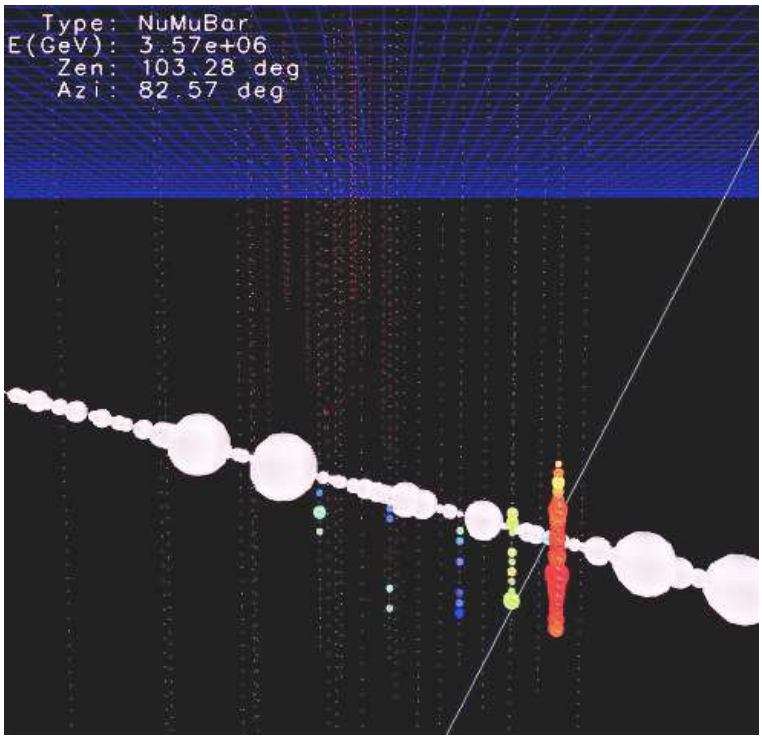

Figure III.9: Example of a muon being detected at IceCube.

reconstructed down going muons that constitute most of the background. Atmospheric neutrinos are the majority of what is detected and provide a very useful calibration sample for AMANDA, but also when searching for extraterrestrial sources of neutrinos they constitute a background. The path of a muon detected in IceCube is shown in Fig. III.9.

For the event yields and discussions presented in this analysis we assume two things. First, the supernova occurs near the center of our galaxy, approximately 10 kpc from earth. Second, from [12], the total energy

release in neutrinos is $3 \times 10^{53} ergs$ and equally divided among the six known neutrinos and anti-neutrinos flavors.

CHAPTER IV

ANALYSIS AND RESULTS

IV.1 Intensity of Neutrinos from a SN

The calculations for the analysis used in this thesis are explained later in this chapter. The following calculations were determined with the most accurate and current values for all constants used in this thesis. We start by calculating the binding energy of a neutron star. For a spherical mass of uniform density the total gravitational binding self-energy U is given by the equation :

$$U = -\frac{3}{5} \times \frac{GM^2}{R} \tag{IV.1}$$

Where G = gravitational constant, M = Mass of sphere, R = radius of the sphere. When examining this energy in greater detail it is safe to visualize this energy as the sum of potential energies. Therefore in order to calculate the potential energy of a shell just on the outside of the enclosed sphere we need to know the masses of both the shell and the sphere contained in it. Upon determining these variables the potentials are then summed up over the entire sphere.

First we assume a constant density ρ, then the masses of the shell and

sphere are given:

$$M_{(shell)} = 4\pi r^2 \rho dr \tag{IV.2}$$

$$M_{(interior)} = \frac{4}{3} \times \pi r^3 \rho \tag{IV.3}$$

Now taking these values and inserting them into Newtons equation for gravitational potential energy

$$dU = -G\frac{M_{(shell)}M_{(interior)}}{R} \tag{IV.4}$$

By integration over the volume of a sphere we get

$$U = -G\int_0^R (4\pi r^2 \rho)(\frac{4\pi r^3 \rho}{3})\frac{dr}{r} \tag{IV.5}$$

$$U = -G\frac{16}{15}\pi^2 \rho^2 R^5 \tag{IV.6}$$

Remember ρ is simply equal to the mass of the whole divided by its volume for objects with uniform densities. Therefore

$$\rho = \frac{M}{\frac{4}{3}\pi R^3} \tag{IV.7}$$

And then finally plugging in the above equation,

$$U = -G\frac{16}{15}\pi^2 R^5 (\frac{M}{\frac{4}{3}\pi R^3})^2 \tag{IV.8}$$

$$U = -\frac{3}{5}\frac{GM^2}{R} \tag{IV.9}$$

U in the above equation is called the self-energy. Using the values for $G = 6.67428 \times 10^{-11} \frac{N.m^2}{kg^2}$, mass of the neutron star ($M_{(star)} = 1.4 M_{(sun)}$ and its radius $R_{(star)} = 10km$. The mass of the sun is equal to $M_{\odot} = 1.98892 \times 10^{30} kg$. Therefore by plugging in these values into the equation IV.9, the binding energy of the neutron star is as follows

$$U = -\frac{3}{5} \frac{G \times M_{(star)}^2}{R_{(star)}} \tag{IV.10}$$

$$U = -\frac{3}{5} \frac{6.67428 \times 10^{-11} \frac{Nm^2}{kg^2} (1.4)^2 (1.98892 \times 10^{30})^2 kg^2}{10km} \tag{IV.11}$$

$$U = 3.105 \times 10^{46} J \tag{IV.12}$$

One Joule is equal to $6.24150974 \times 10^{12}$ MeV. The binding energy is $U = 1.937921 \times 10^{59}$ MeV. This value which can be divided by the number of neutrino and antineutrino flavors to yield the energy of $E_N = 3.22987 \times 10^{58}$ MeV per species.

The average neutrino energy for each flavor is given as stated in Balantekin and Yuksel,"Neutrino mixing and nucleosynthisis in core-collapse supernovae" [6]:

$$E_{(\nu_e)} = 10 MeV \tag{IV.13}$$

$$E_{(\bar{\nu}_e)} = 15 MeV \tag{IV.14}$$

$$E_{(\nu_x, \bar{\nu}_x)} = 24 MeV \tag{IV.15}$$

Now taking these energies and dividing the total energy by the energy of each particular flavor. The total number of neutrinos in each flavor is computed.

$$N_{(\nu_e)} = \frac{E_N}{10MeV} = 3.2299 \times 10^{57} \tag{IV.16}$$

$$N_{(\bar{\nu}_e)} = \frac{E_N}{15MeV} = 2.1532 \times 10^{57} \tag{IV.17}$$

$$N_{(\nu_x,\bar{\nu}_x)} = \frac{E_N}{24MeV} = 1.3458 \times 10^{57} \tag{IV.18}$$

With the total number of neutrinos per flavor the intensity can be computed using the following equation.

$$Intensity = I = \frac{Total\ number\ of\ neutrinos}{Total\ Area} \tag{IV.19}$$

The area of a sphere $A_{sphere} = 4\pi D^2$, where D is the distance from the star to earth (10kpc) contains all the neutrinos due to the exploding SN. One parsec is equal to 3.26 light years or $3.08568025 \times 10^{18}$cm and radius 10 kpc is equal to $3.08568025 \times 10^{22}$cm. Therefore the total area covered is $A_{sphere} = 1.195 \times 10^{46} cm^2$ The flux for each flavor of neutrino that would be seen in the IceCube detector during 10 seconds can easily be calculated as follows.

$$I_{(\nu_e)} = 2.7134 \times 10^{11} cm^{-2} \tag{IV.20}$$

$$I_{(\bar{\nu}_e)} = 1.8094 \times 10^{11} cm^{-2} \tag{IV.21}$$

$$I_{(\nu_x,\bar{\nu}_x)} = 1.1309 \times 10^{11} cm^{-2} \tag{IV.22}$$

Neutrino oscillations between SN and earth will equlize the number of each flavor in both matter an antimatter sectors. In other words, the total average

number of electron antineutrinos used in this thesis is $(2\times1.1309\times10^{11}cm^{-2}+1.8094\times10^{11}cm^{-2})/3 = 1.3571\times10^{11}cm^{-2}$

IV.2 Natural Abundance of Isotopes

Here we look at the natural abundance of isotopes found in the one km^3 of ice that composes the IceCube detector. In the ice we have $O^{16}, O^{17}, O^{18}, H^1$, and H^2 all isotopes that make up the ice that house the IceCube detector. Taking the density of the ice $\rho_{(ice)} = 0.9167g/cm^3$ and the mass of the ice M_{ice} = Volume $\times\rho_{(ice)} = 0.9167\times10^{15}$ g. This we use in determining the mass of each molecule by multiplying the mass times the natural abundance.

$$M_{(H_2O^{16})} = M_{(ice)}\times(0.99762) = 9.1452\times10^{14} \tag{IV.23}$$

$$M_{(H_2O^{17})} = M_{(ice)}\times(0.00038) = 3.4835\times10^{11} \tag{IV.24}$$

$$M_{(H_2O^{18})} = M_{(ice)}\times(0.002) = 1.833\times10^{12} \tag{IV.25}$$

The number of moles (N) is equal to the natural abundance divided by the atomic mass of the molecule.

$$N_{(H_2O^{16})} = \frac{M_{(H_2O^{16})}}{18.011} = 5.0776\times10^{13} \tag{IV.26}$$

$$N_{(H_2O^{17})} = \frac{M_{(H_2O^{17})}}{19.015} = 1.832\times10^{10} \tag{IV.27}$$

$$N_{(H_2O^{18})} = \frac{M_{(H_2O^{18})}}{20.1592} = 9.0926\times10^{10} \tag{IV.28}$$

The total number of molecules is the total number of moles times Avogadro's number which is equal to $N_A = 6.0221415\times10^{23}$

$$H_2O^{16} = N_{(H_2O^{16})}N_A = 3.0578\times10^{37} \tag{IV.29}$$

Table 1: Shows the different isotopes and electrons found in the IceCube.

Isotope	Atomic mass	Natural Abundance	Number of Atoms
O^{16}	15.995	0.99762	3.056×10^{37}
O^{17}	16.999	0.00038	1.102×10^{34}
O^{18}	17.9992	0.002	5.477×10^{34}
H^1	1.008	0.99985	6.124×10^{37}
H^2	2.014	0.0115	7.044×10^{35}
e	0.0	0.0	3.06×10^{38}

$$H_2O^{17} = N_{(H_2O^{17})}N_A = 1.1033 \times 10^{34} \tag{IV.30}$$

$$H_2O^{18} = N_{(H_2O^{18})}N_A = 5.4757 \times 10^{34} \tag{IV.31}$$

The number of molecules multiplied by two and total the sum to get the number of Hydrogen atoms in the IceCube $H_{atoms} = 6.1288 \times 10^{37}$. Multiplying H_{atoms} by the natural abundance will yield the total number of hydrogen isotopes in the ice. The natural abundance of $H^1 = 99.9885\%$ and $H^2 = 0.115\%$ give the total number of atoms of $H^1 = 6.1281 \times 10^{37}$ and $H^2 = 7.0481 \times 10^{34}$.

The image IV.1 is of SN 1987A, the closest SN to be observed by anyone since SN1604.

IV.3 Cross Section Calculations

The "cross section" is the likelihood of interaction between particles in nuclear and particle physics. If a projectile is aimed at a solid target in

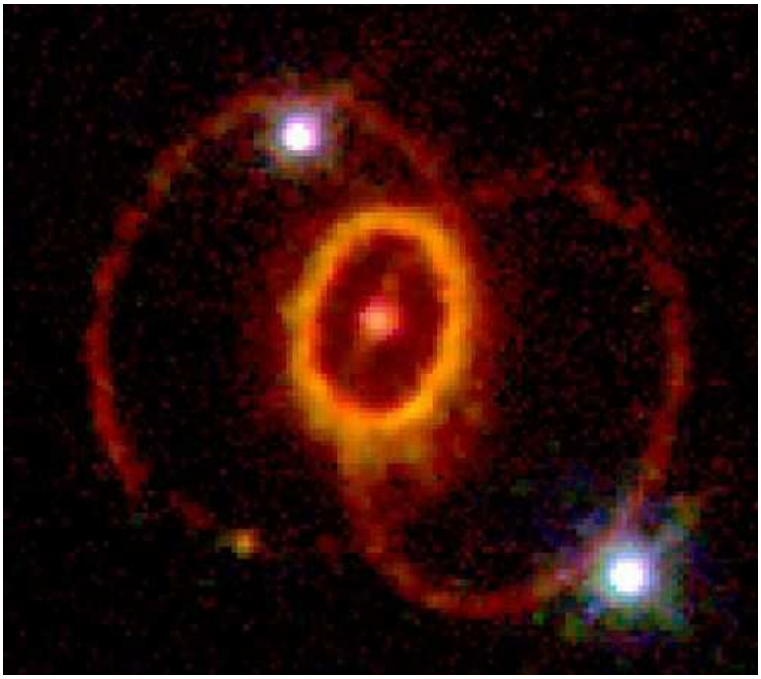

Figure IV.1: SN 1987A was a supernova in the outskirts of the Tarantula Nebula in the Large Magellanic Cloud, a nearby dwarf galaxy (≈ 51.4 kpc). It occurred so close to the Milky Way that it was visible to the naked eye and it could be seen from the Southern Hemisphere. It was the closest observed supernova since SN 1604, which occurred in the Milky Way itself. The light from the supernova reached Earth on February 23, 1987. As the first supernova discovered in 1987, it was labeled "1987A".

a specified region and hits the solid target, we assume that this interaction will occur with 100% probability. But if the projectile does not hit the solid target, this interaction is said to have 0% probability. Therefore to compute the total interaction probability for a single projectile to hit a solid target will be determined by taking the ratio of the number of hits by the projectile in the area of the solid (the cross section) to the number of hits in the total targeted region. This basic concept to used to determine this interaction may be extended to cases where the interaction probability in the targeted area assumes intermediate values. These values ranging from the target itself not being homogeneous or the interaction being mediated by a non-uniform field. The differential cross section is defined as the probability to observe a scattered particle in a given quantum state per solid angle unit within a given cone of observation, if the target is irradiated by a flux of one particle per surface unit.

The $\bar{\nu}_e p \rightarrow n e^+$ reaction cross section is very difficult to measure experimentally. At low energies in the reactor energy range, the $\bar{\nu}_e$ have an average energy of a few MeV [21] and are much lower in energy than the SN neutrinos. At pion factory such as the old factories where pions are copiously produced such as the old Los Alamos Meson Physics Facilty (LAMPF), the $\bar{\nu}_e$'s can only be the product of the π^- decay that are captured in the target when they come to rest. This will make it virtually impossible to measure this cross section. We, therefore, have to rely solely on calculations for the above cross section.

	E_ν, MeV	5	10	16*	20	40	80
1	Naive	0.02	0.08	0.21	0.33	1.32	5.28
2	Naive +	0.02	0.07	0.19	0.29	1.16	4.64
3	Vogel and Beacom	0.12	0.07	0.19	0.29	0.98	2.31
4	Strumia and Vissani	0.12	0.07	0.19	0.29	0.98	3.17
5	Horowitz	0.022	0.09	0.24	0.33	1.12	3.3
6	Llewellyn-Smith+	0.012	0.07	0.19	0.29	1.04	3.22
7	LS + VB	0.012	0.07	0.19	0.29	1.04	3.22
8	Gaisser and O'Connell	0.03	0.12	0.31	0.48	1.92	7.68

Table 2: *Various approximations for* $\sigma(\bar{\nu}_e p \to n\bar{e})$ *in units of* $10^{-40} cm^2$ * *represents SN neutrino energy.*

Table 2 shows the cross section calculation from different authors. In the following calculations we define $\delta = m_n - m_p \approx 1.293$ MeV and M $= (m_n + m_p)/2 \approx 938.9$ MeV. In the table we consider the $\bar{\nu}_e$ reaction.

1. The **naive** low-energy approximation (see e.g.[18])

$$\sigma \approx 9.52 \times 10^{-44} \frac{p_e E_e}{\mathrm{MeV}^2} \ \mathrm{cm}^2, \qquad E_e = E_\nu \pm \Delta \text{ for } \bar{\nu}_e \text{ and } \nu_e, \quad \text{(IV.32)}$$

obtained by normalizing the leading-order (LO) result to the neutron lifetime, overestimates $\sigma(\bar{\nu}_e p)$ especially at high energy.

2. A simple approximation which agrees with our full result within a few per-million for $E_\nu \leq 300$ MeV is

$$\sigma(\bar{\nu}_e p) \approx 10^{-43} \,\mathrm{cm}^2 \ p_e E_e \ E_\nu^{-0.07056 + 0.02018 \ln E_\nu - 0.001953 \ln^3 E_\nu}, \quad \text{(IV.33)}$$

$$E_e = E_\nu - \Delta \quad \text{(IV.34)}$$

where all energies are expressed in MeV.

3. The low-energy approximation of **Vogel and Beacom** [16] (which include first order corrections in $\varepsilon = E_\nu/m_p$, given only for anti-neutrinos) is very accurate at low energies ($E_\nu < 60$ MeV), however underestimates the number of supernova IBD neutrino events at highest energies by 10%. Higher order terms in ε happen to be dominant already at $E_\nu > 135$ MeV, where the expansion breaks down giving a negative cross-section [16, 19].

4. The **Strumia and Vissani**[13] low-energy approximation, defined by the equation:

$$\begin{aligned} A &\simeq M^2(f_1^2 - g_1^2)(t - m_e^2) - M^2\Delta^2(f_1^2 + g_1^2) \; - 2m_e^2 M\Delta g_1(f_1 + f_2) \\ B &\simeq t \; g_1(f_1 + f_2) \\ C &\simeq (f_1^2 + g_1^2)/4 \end{aligned} \tag{IV.35}$$

   can be used from low energies up to the energies relevant for supernova $\bar{\nu}_e$ detection. They expand the squared amplitude in ε but, unlike Vogel and Beacom, they treat kinematics exactly, so that some higher order terms are included in the Strumia and Vissani cross section. In above equations, M is the average mass of a neutron-proton pair, $f_1 = 1$ is the vector coupling constant, $f_2 = 3.71 f_1/2M$, $g_1 = 1.272 \pm .002$ is the axial vector coupling constant, and $t = m_n^2 - m_p^2 - 2m_p(E_\nu - E_e)$.

5. The high-energy approximation of **Horowitz** [19], obtained from the Llewellyn-Smith formulae[14] setting $m_e = 0$, was not tailored to be used below ~ 10 MeV, and it is not precise in the region relevant for supernova neutrino detection; however, it is presumably adequate to describe supernova neutrino transport.

6. The **Llewellyn-Smith** high-energy approximation, improved adding $m_n \neq m_p$ in s, t, u, but not in $\mathcal{M}$ is very accurate at all energies relevant for supernova neutrinos, failing only at the lowest energies. As proved previously, this is a consequence of the absence in $|\mathcal{M}^{\in}|$ of corrections of order Δ/m_p.

7. Approximation 6. can be improved by including also the dominant low-energy effects in the amplitude $\mathcal{M}$, as discussed in section IIB of [16].

8. The **Gaisser and O'Connell** formalisim was used to produce the results shown in figure IV.2.

   In this figure, we show the distribution of the different neutrino concentrations within the neutrinosphere. The emitted positrons after intercation in the IceCube was generated with the formalisim of Gaisser and O'Connell[2]. Also shown for comparison are the data form the detected events of IMB and Kamioka for SN1987A.

IV.4 Detector Sensitivity to SN Explosion

The intensity times the inverse β-decay cross section (0.31×10^{-40}) and the number of protons (6.13×10^{37}) yields the number of positrons generated in the detector which is $N_{e^+} = 2.60 \times 10^8$. A GEANT-3.21 calculation [20] with the IceCube geometry and the DOM quantum efficiency with layered ice yields an efficiency of 0.0075 for production of photoelectrons (PE). This gives 1.95×10^6 DOM hits in a 10-second interval. To obtain the total noise for the same 10-second time interval

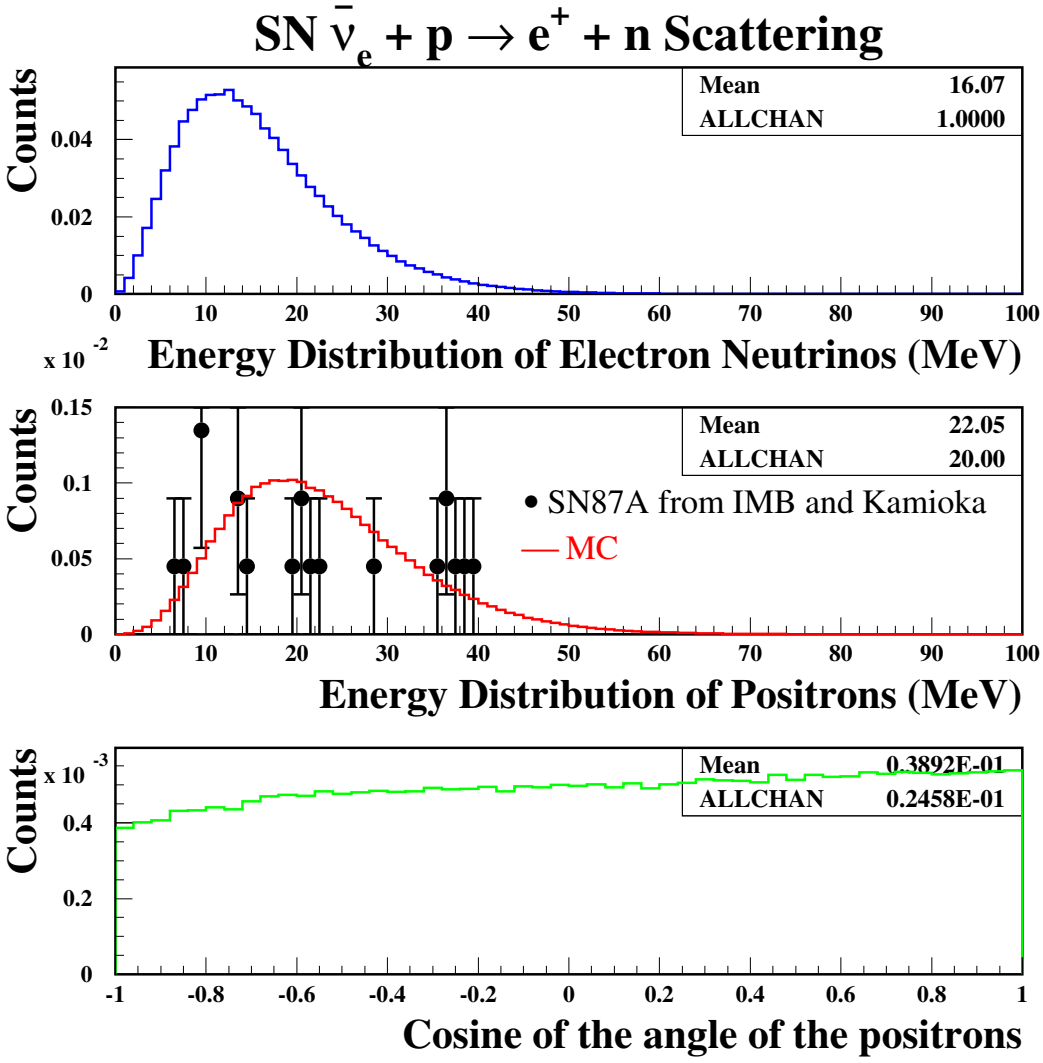

Figure IV.2: Comparison of the energy distribution of the Supernova Electron Neutrinos that of the Positrons during $\bar{\nu_e} + p \rightarrow e^+ + n$ scattering in MeV.[1]

of all 4800 DOMs, we multiply number of DOMs by the time $\Delta t = 10$ sec and the dark rate of 300 Hz, Therefore,

$$DetectorNoise = 4800 \times 300 \times 10 = 1.44 \times 10^7 \tag{IV.36}$$

This value gives rise to a statistical fluctuation of σ equal to ± 3800. In turn yields a value of 513σ that when divided by 5.5σ (IceCube trigger) is 93. Solving the equation below gives the distance that the detector will be sensitive to

$$\frac{R^2}{100} = 93 \tag{IV.37}$$

$$R^2 = 9300 \tag{IV.38}$$

$$R = 97kpc. \tag{IV.39}$$

In the figures IV.3,IV.4, we show the range of sensitivity for the IceCube detector using the values shown in the table 3. The figure IV.5 shows a 3-D representation of the Milky Way along with its nearest neighboring galaxies.

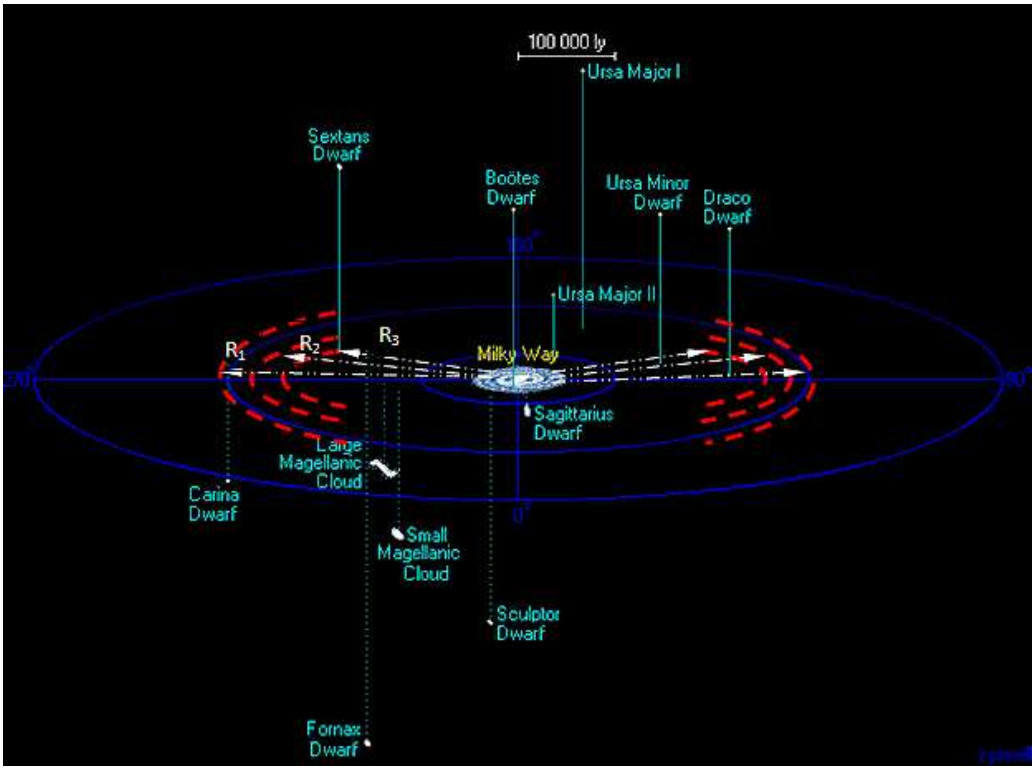

Figure IV.3: Schematic view showing the range of the sensitivity of the IceCube detector along with corresponding authors calculations of sensitivity in our galactic neighborhood. The values for the corresponding radius are $R_1 = 97$ kps, $R_2 = 86$ kpc, and $R_3 = 76$ kpc, corresponding to cross sections from Gaisser and O'Connell, Horowitz, and (Naive +, Vogel and Beacom, Srumia and Vissani, Llewellyn-Smith +, and LS+VB), respectively. Each shown radius can be visualized as having an spherical shape surrounding the galactic neighborhood. Not shown in the above picture is the Naive model that yields a sensitive radius of 79 kpc.[22]

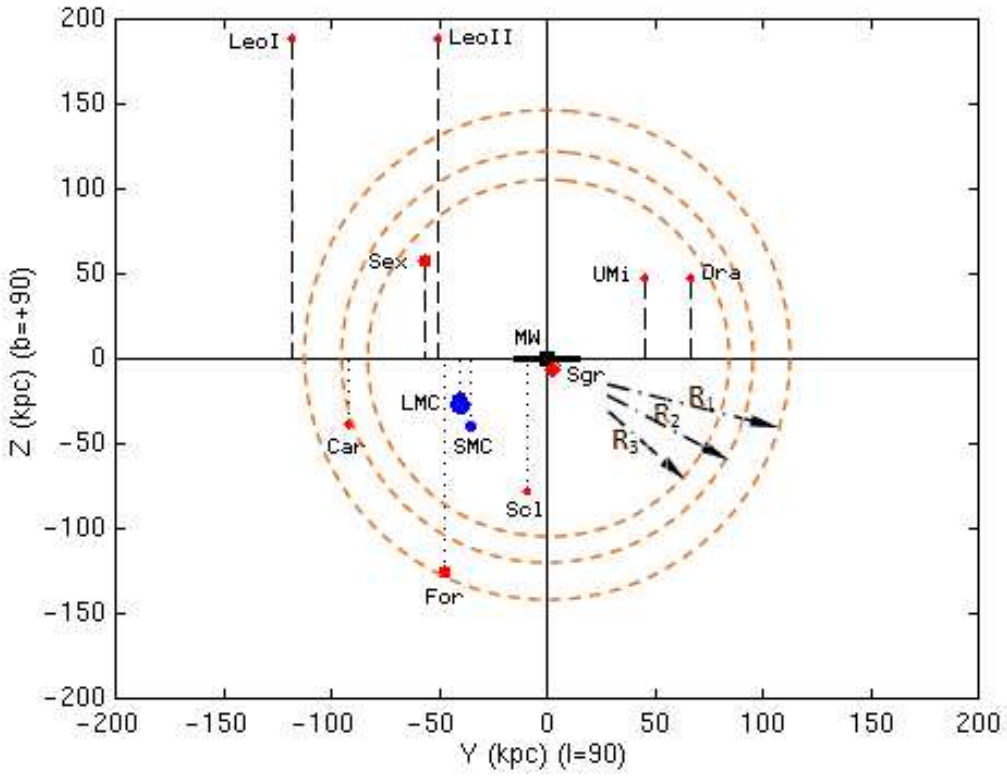

Figure IV.4: Schematic top view showing the range of sensitivity of the IceCube detector along with the same corresponding values for R_1, R_2, and R_3 as stated in the previous figure IV.3.[23]

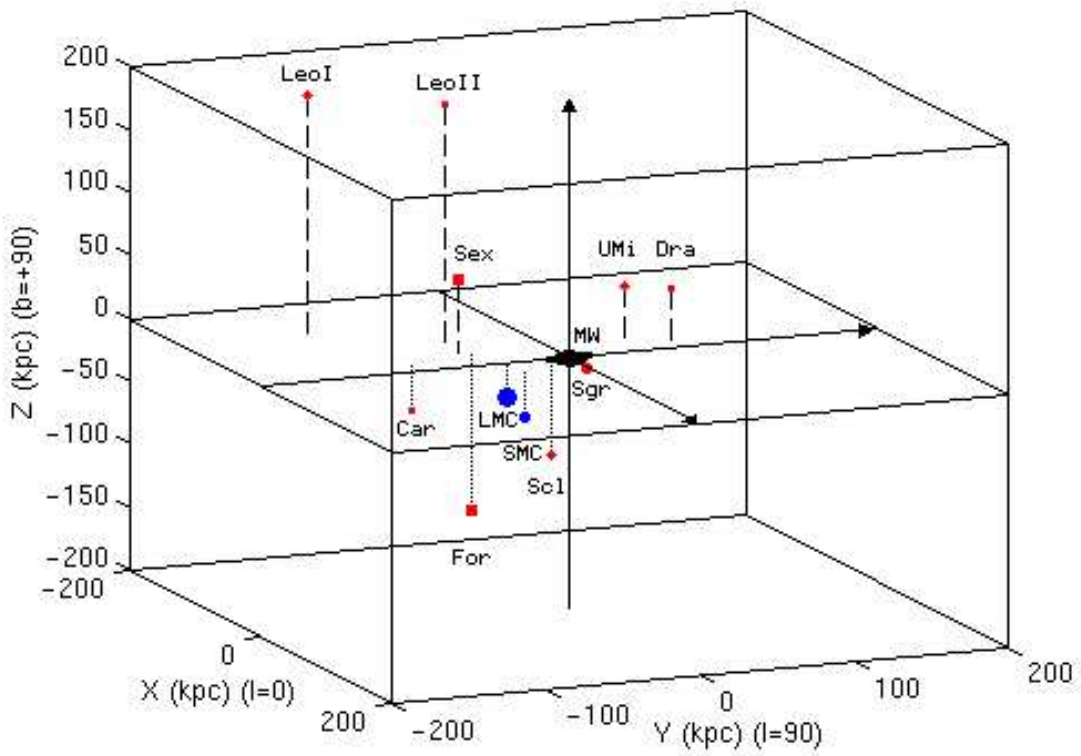

Figure IV.5: 3-D view of Milky Way and neighboring galaxies.[23]

Table 3: Sensitivity of detection with different authors' calculations

Author	$\sigma(\bar{\nu}_e p \rightarrow n e^+)$	Distance (kpc)
Naive	0.21	79
Naive +	0.19	76
Vogel and Beacom	0.19	76
Strumia and Vissani	0.19	76
Horowitz	0.24	86
Llewellyn-Smith +	0.19	76
LS + VB	0.19	76
Gaisser + O'Connell	0.31	97

CHAPTER V

CONCLUSIONS

In summary, we have studied several cross section calculations for $\bar{\nu}_e p \rightarrow ne^+$ reaction. This neutrino interaction dominates all other reactions in a future SN explosion detected by the IceCube detector. The cross section calculations are the only tools that we have at our disposal at this energy range, since this cross section cannot be measured experimentally. At low energies in the reactor energy range, the $\bar{\nu}_e$ has an average energy of a few MeV [21] and are much lower in energy than the SN neutrinos. At pion factories where pions are copiously produced such as the old LAMPF, the $\bar{\nu}_e$'s can only be the product of the π^-'s decay that are captured when they come to rest in the target. This will make it practically impossible to measure this cross section. We have calculated the cross section at the SN energy to be $0.19 \times 10^{-40} cm^2$ with the Naive +, Vogel and Beacom, Strumia and Vissani, Llewellyn-Smith, and LS+VB models. The Naive model yields $0.21 \times 10^{-40} cm^2$, with $0.24 \times 10^{-40} cm^2$ for Horowitz and $0.31 \times 10^{-40} cm^2$ for the Gaisser and O'Connell cross sections.

These values lead to the range of sensitivity for the IceCube detector to be determined as 76 kpc, 79 kpc, 86 kpc, and 97 kpc respectively for the given

authors. These sensitivities make the IceCube detector the most sensitive SN antenna in the world.

BIBLIOGRAPHY

[1] These GEANT calculations were performed by Ali R. Fazely.

[2] T.K. Gaisser and J.S. O'Connell, Interactions of atmospheric neutrinos on nuclei at low energy, Phys. Rev. D 34 3 p822 (1986)

[3] M. Liebendorfer, et al., Phys. Rev. D 63 103004 (2001)

[4] Amol S. Dighe, Mathis Th. Keil and Georg G Raffelt, hep-ph/0303210v3 (2003), JCAP 0306, 005 (2003).

[5] W. Pauli, Letter to the Physical Institute of the Federal Institute of Technology (ETH), unpublished, (December 1930)

[6] A. B. Balantekin and H. Yuksel, New Journal of Physics 7 (2005)

[7] V. Barger, D. Marfatia and B.P. Wood, arXiv:hep-ph/0112125v3 (2002), Phys. Lett. B547, 37-42 (2002).

[8] M. Ackermann et al., J of Geophys. Res. v111, D13203 (2006).

[9] $http://wiki.icecube.wisc.edu/index.php/GEANT/IceSim_comparison$

[10] V. Flaminio, ANTARES Collaboration, Proc Sci. HEP2005 (2006) 25

[11] R. Buras, H-T Janka, arXiv:astro-ph/0205006v1 (2002),Astrophys.J. 587, 320-326 (2003.

[12] Kate Scholberg, arXiv:hep-ex/0008044v1 (2000), Nucl. Phys. Proc. Suppl. 91, 331-337 (2000).

[13] A. Strumia and F. Vissani, arXiv:astro-ph/0302055 v2 (29 Apr 2003), Phys.Lett. B564, 42-54 (2003).

[14] C.H. Llewellyn-Smith, Phys. Rep. 3 261 (1972).

[15] Suzuki H 1993 Proc. Int. Symp. on Neutrino Astrophysics ed Y suzuki and K. Nakamura (Tokyo: Universal Acadamy Press)

[16] P. Vogel and J.F. Beacom, Angular distribution of neutron inverse beta decay, $nubar_e + p \rightarrow (e^+) + n$,The American Physical Society (1999)

[17] H.M. Gallagher and M.C. Goodman, Neutrino Cross Sections, NuMI-112 PDK-626 (Nov. 10, 1995)

[18] C. Bemporad, G. Gratta and P. Vogel, Rev. Mod. Phys. 74 (2002) 297

[19] C.J. Horowitz, Phys. Rev. D 65 (2002) 043001.

[20] A. R. Fazely, Private Communications, (2008)

[21] H. Murayama and A. Pierce, arXiv:hep-ph/0012075v3 (2000), Phys.Rev. D65, 013012 (2002).

[22] http://www.astro.uu.se/ ns/mwsat.html

[23] http://www.atlasoftheuniverse.com/sattelit.html

VITA

Aaron Simon Richard was born in Baton Rouge, capitol city of Louisiana, on the 2nd day of September in 1969. He graduated from McKinley Senior High School in 1987. Upon completing requirements for Bachelor of Science in Physics he was awarded his degree in May of 1995. After a short leave, he was admitted to the Master of Science program at Southern University in 1999 to pursue his career in Physics.

APPROVAL FOR SCHOLARLY DISSEMINATION

The author grants to the Souther University Library the right to reproduce, by the appropriate methods, upon request, any or all portions of this thesis.

It is understood that "request" consists of an agreement on the part of the requesting party, that said reproduction will not occur without written approval of the author of this thesis.

The author of this thesis reserves the right to publish freely, in the literature, at any time, any or all the portions of this thesis.

Author _____

Date _____